



Electrical properties and impedance spectroscopy of crystallographically textured 0.675 [Pb(Mg_{1/3}Nb_{2/3})O₃]-0.325 [PbTiO₃] ceramics

Ayşe Berksoy-Yavuz¹ · Ebru Mensur-Alkoy¹

Received: 26 February 2018 / Accepted: 8 June 2018 / Published online: 14 June 2018
© Springer Science+Business Media, LLC, part of Springer Nature 2018

Abstract

Crystallographically (001)-textured lead magnesium niobate (PMN)—lead titanate (PT) solid solution in the ratio of 0.675PMN-0.325PT was fabricated by tape-casting method using barium titanate (BaTiO₃-BT) templates. Random PMN-PT with the same composition was also produced by tape-casting method for comparison. According to electromechanical and dielectric investigations, textured PMN-PT ceramics produced at 1150 °C for 2 h in oxygen atmosphere with 1 vol% BT were found to display the optimum properties. Dielectric constant, dielectric loss and piezoelectric coefficient of these samples were found to be as 1950, 0.002 and 700 pC/N, respectively. The impedance spectroscopy of the samples was conducted and the results of measurements taken at 300 and 500 °C were compared. A significant decrease in the electrical conductivity was observed with the development of texture in PMN-PT. The slightly depressed semicircles that were obtained from Nyquist diagrams indicated non-Debye-type relaxation with a distribution of relaxation time.

1 Introduction

Lead zirconate titanate [Pb(Zr_xTi_{1-x})O₃ or PZT] was to become the mainstream material in the commercial electronic device industry after its discovery at early 1950s in Japan [1, 2]. PZT ceramics exhibit extraordinarily large piezoelectric and electromechanical properties around the morphotropic phase boundary (MPB) between rhombohedral 3 m, tetragonal 4 mm and monoclinic m phases. Piezoelectrics have many specific and important application areas in today's technology. They can be used in energy harvesting area especially in micro electro mechanical systems (MEMS)-scale to create power for electronic devices directly such as cellular phones and communicators. Piezoelectric strain constant (d) and piezoelectric voltage constant (g) are very important and values of them should be high for actuating and sensing. The power density, output voltage, and operational bandwidth are for also vital energy harvesting. Additionally, energy conversion efficiency is the most important issue when designing piezoelectric MEMS energy

harvesters. The figure of merit (FOM) of MEMS-scale harvesters for a given material of fixed sizes can be calculated with a material with high (d.g) product. Thus, high power will be produced when the piezoelectric ceramic is directly employed for energy harvesting [3, 4].

PZT ceramics can also be easily adapted to the requirements of different applications by cation modification into the A and/or B site of ABO₃ perovskite structure [5, 6]. The piezoelectric properties can be further enhanced in a single crystal form of the same composition, although the growth of single crystal PZT is very difficult, due to the incongruent melting of PZT owing to the much higher melting point of ZrO₂ [2]. Single crystals are highly anisotropic in certain directions. Anisotropy also directly affects elastic, dielectric and piezoelectric properties [7, 8]. Thus, great deals of effort have been spent to develop new single crystal systems for device design which exhibit high performance [8–10]. (001) oriented single crystals of (1-x)Pb(Mg_{1/3}Nb_{2/3})O₃-xPbTiO₃ (PMN-PT), was firstly reported by Park and Shrout [8, 9, 11]. They have received increasing attention due to their outstanding 33-mode piezoelectric and electromechanical performance (d₃₃ ~ 1500–2500 pC/N, k₃₃ > 94%, strain > 0.7%), which are much higher than the commercial PZT ceramics [8–10]. This is due to the ease of orientation of domains in single crystals during poling process, so that the maximum performance can be obtained. Single crystal PMN-PT

✉ Ebru Mensur-Alkoy
ebrualkoy@gtu.edu.tr

¹ Department of Materials Science and Engineering, Gebze Technical University, 41400 Gebze, Kocaeli, Turkey

shows higher strain than soft PZT, in addition to having less hysteretic behavior than hard PZT and it is also suitable for actuator and transducer applications [8–10]. Especially, 0.675Pb(Mg_{1/3}Nb_{2/3})O₃-0.325PbTiO₃ composition near morphotropic phase boundary in single crystal form exhibit high piezoelectric properties due to intermediate coexisting phases. From the binary phase diagram of PMN and PT, monoclinic dominant mixed phases which the polarization can easily follow along the applied field resulting in high piezo response was reported in the range 31–37% PT [3, 9].

However, device applications of single crystals are limited because of high- production cost, long growth time, small size and compositional heterogeneity across the ingot. In order to overcome these major problems, fabrication of textured relaxor piezoelectric ceramics using combination of templated grain growth (TGG) and tape casting methods came into prominence to enhance the piezoelectric properties, which are comparable to single crystals, while the cost of production is comparable to the polycrystalline ceramics [3, 12–15]. Tape casting method enables fabrication of ceramics in the intended shape and size. The perovskite plate-like BaTiO₃ (BT), SrTiO₃ (ST) and (Na_{1/2}Bi_{1/2})TiO₃-PbTiO₃ (NBT-PT) template particles with lattice parameters that are similar to the matrix are used for texturing of PMN-PT ceramics [12, 16–18]. The selection of template particles and their amount generally affects the degree of crystallographic texture, electrical and dielectric properties [15–18]. For example, while textured PMN-PT reached a high degree of orientation using SrTiO₃ templates, the Curie temperature (T_c) shifted to a lower temperature (from 132 to 100 °C) and the maximum dielectric constant (ε_{max}) decreased because of the low depolarization temperature (~60 °C) and dissolution of Sr²⁺ in PMN-PT matrix [17]. Since the BT templates are generally stable in the PMN-PT matrix, residual templates cause clamping effects due to the stresses that arise between the template and the matrix and this may adversely affect electrical properties with increasing BT content [12, 14, 18, 19]. Electrical and dielectric properties of ferroelectric oxides also depend on the defect concentration in the structure and this can be discussed through the electronic and ionic conductivity [19–21]. Impedance spectroscopy is the most effective technique for determination of AC conductivity as a function of frequency and temperature. Impedance (Z*) has two parts that are real (Z') and imaginary (Z''). Real and imaginary parts are explained by resistance (R) and capacitance (C) and the relation can be expressed as

$$Z^* = [R^{-1} + j\omega C]^{-1} \quad (1)$$

where ω is the angular frequency ($\omega = 2\pi f$) of the AC field and $j = \sqrt{-1}$. The frequency dependence of the electrical properties of a material can be described in terms of the complex impedance Z*, complex admittance Y*, the

complex permittivity ϵ^* , and the dielectric loss or the dissipation factor $\tan \delta$. They are infact interrelated to one another. Impedance data gives a semicircle when Z'' versus Z' is plotted and this diagram is called the Nyquist diagram. Impedance plots exhibit two semi-circle that are attributed to grain and interfacial grain boundary phases [20–23].

In this work, (001) oriented 0.675Pb(Mg_{1/3}Nb_{2/3})O₃-0.325PbTiO₃ binary ceramic composition was chosen to be fabricated by the TGG approach using plate-like BT template in various ratios. The main purpose and the contribution to the literature of the study were to investigate the optimum processing conditions and template ratio to achieve high figure of merit for potential energy harvesting applications. To explain the effect of these parameters on the electrical properties of PMN-PT, detailed experimental study was conducted. As another original contribution, electrical properties were considered in the case of FOM and systematically reported with respect to the processing conditions, and impedance spectroscopy was used to explain the effect of BT on the dielectric properties of PMN-PT.

2 Experimental procedure

Textured 0.675Pb(Mg_{1/3}Nb_{2/3})O₃-0.325PbTiO₃ (0.675PMN-0.325PT) ceramics were fabricated by the TGG method using various ratios of BT templates. PMN-PT powders were prepared by columbite precursor method to eliminate pyrochlore phase. The raw materials Pb₃(CO₃)₂(OH)₂ (Sigma-Aldrich, Germany), TiO₂ (Degussa, Denmark) and MgNb₂O₆ (synthesized at 1150 °C for 4 h) [24] were weighed according to stoichiometric ratio and ball-milled for 24 h in polyethylene bottle with mixed 3–5 mm yttria stabilized ZrO₂ (YSZ) balls (Inframat Advanced Materials, USA). This mixture was dried at 60 °C and calcined at 750 °C (heated with a rate of 5 °C/min) for 2 h and then 2 wt% excess PbO was added in the crushing stage for compensation of lead loss during sintering. It was dried again at 60 °C.

Plate-like BT templates were synthesized by a two-stage molten salt (MSS) synthesis and topochemical microcrystal conversion method (TMC). In first and second stages, precursor Bi₄Ti₃O₁₂ (BiT) and BaBi₄Ti₄O₁₅ (BBT) templates were prepared using molten salt method. Finally, BT templates were synthesized by mixing BBT particles with BaCO₃ (Alfa Aesar, Germany) and using KCl (Merck, Germany) as a flux. The mixture was then heated at 950 °C for 3 h in covered alumina crucible to prevent Bi volatilization. The final product was washed using diluted HNO₃ acid solution (65%, Merck) to remove bismuth oxide (Bi₂O₃) by-product and residual KCl was separated from BT templates by washing in hot deionized water and thus, the pure plate-like BT templates were obtained [3, 25–27]. The BT

templates added in to the PMN-PT matrix powder were used to enhance the degree of grain orientation and electrical properties in samples. The slurries for tape casting were prepared by ball-milling the calcined matrix powder with organic binder and methyl ethyl ketone/ethanol solvents. BT templates were mixed in the slurries with a magnetic stir bar for 24 h. The final viscosity of the slurry was measured as 200 mPa s at 500 1/s shear rate. Afterward, stable slurries were casted at the rate of 10 cm/min by using doctor blade height of 200 μm . After drying process, the green tapes were cut and stacked into a disk shape of 16 mm diameter and pressed by uniaxial press under 80 MPa. Prior to sintering, the binder and organic solvent of samples were first removed at 600 °C for 1 h in air with heating rates of 1 °C/min. The laminated green samples were sintered at various temperatures such as 1150, 1200 and 1250 °C for 2, 6 and 10 h with 5 °C/min heating rate in air or under O₂ atmosphere (0.2 L/min) in tube furnace. The samples fabricated with 0, 1, 3, 5 vol% BT addition were abbreviated as P0T, P1T, P3T and P5T, respectively. Random samples without any template particles have also been fabricated for comparison. The correlation between the degree of texture and the electromechanical and the dielectric properties were simultaneously investigated in detail. Samples were prepared with approximately 1 mm thickness.

The phase analysis was done by X-ray diffraction-XRD (Bruker D8 Advanced, Germany) using Cu-K α radiation in the 2 θ range from 20° to 60° with a step size of 0.02°. The grain orientation in the ceramics was evaluated from the XRD patterns using Lotgering factor (*f*) method and was used as a semiquantitative degree of texture [28]. Microstructural examination of thermally etched surface was carried out by Philips XL30 scanning electron microscope-SEM (FEI Co., USA). The parallel circular surfaces of the samples were coated with silver paste electrode and fired at 600 °C for electrical measurements. The hysteresis loops of samples were obtained using a Precision LC ferroelectric tester (Radiant Technologies, Inc., USA). The samples were poled in a silicon oil bath at 80 °C by applying a DC electrical field of 30 kV/cm for 15 min. The dielectric constant and loss of ceramics were measured using Hioki 3520 LCR meter (Hioki, Japan) at 10 kHz in a temperature range of 25–250 °C at 2 °C/min. Hysteresis loops were evaluated by a Precision LC ferroelectric tester (Radiant Technologies, Inc., USA) and the electric-field induced strain behaviors were determined using MTI 2000 photonic sensor (MTI Instrumet Inc., USA) at room temperature. The direct piezoelectric coefficients (d_{33}) were also measured by a d_{33} meter (APC International Ltd., USA) after aging for 24 h. Figure of merit (FOM) for energy harvesting applications was calculated as piezoelectric voltage coefficient (g_{33}) \times piezoelectric charge coefficient (d_{33}). Impedance/gain phase analyzer was used to obtain impedance spectrum (E4990A Impedance Analyzer

Keysight Technologies) over frequencies from 100 Hz to 10 MHz in a temperature range of 25–500 °C. The densities of the samples were measured by the Archimedes method. The densities of the all samples sintered under O₂ rich atmosphere were found to be as ~95–98% of the theoretical density (8.1 g/cm³). The flow chart of the whole process was given Fig. 1.

3 Results and discussion

3.1 Structural and electrical properties

In this study, the precursor PMN-PT powders were synthesized by solid-state calcination method following the columbite precursor route. From the XRD analyses of the powders calcined at 750 °C for 2 h, pure perovskite phase was observed without the presence of a secondary phase (not given here). The particle size of the PMN-PT powders was measured to be mostly in the 3–4 μm range with a small fraction under 1 μm .

The XRD pattern and SEM micrograph representative of the BT templates were also given in Fig. 2. The XRD pattern was indexed according to pseudocubic structure but peak splitting observed at $2\theta \approx 45^\circ$ was indexed according to tetragonal structure. From the XRD pattern in Fig. 2a, the templates are crystallized in pure perovskite phase and any

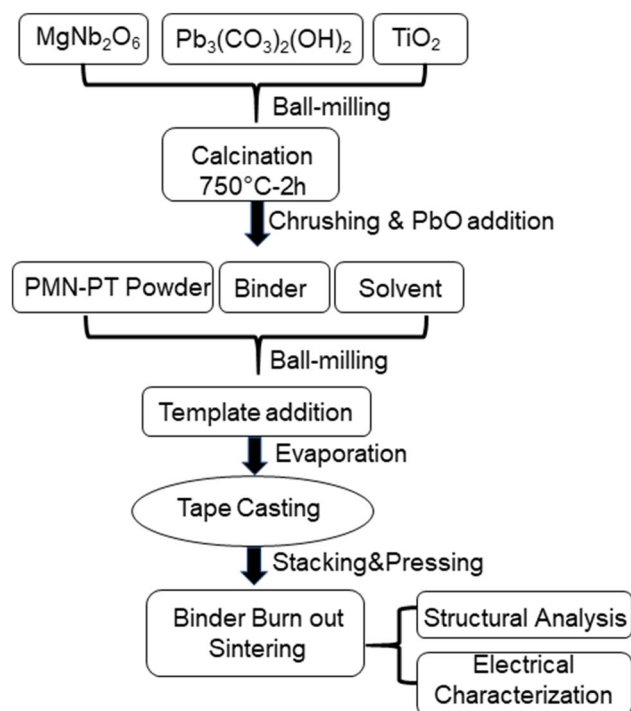


Fig. 1 The process and characterization flow chart of ceramic samples

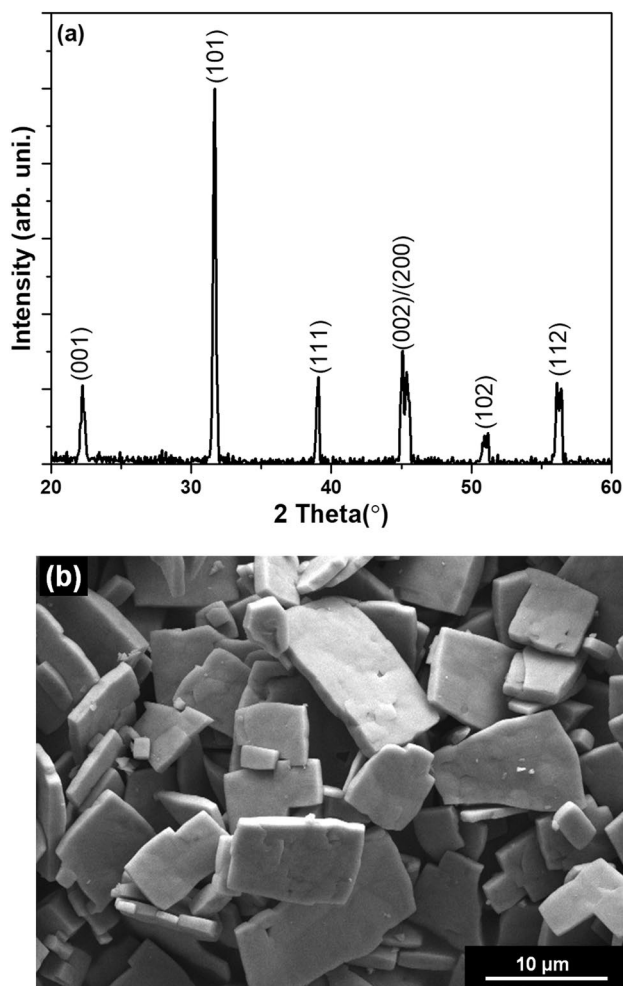


Fig. 2 **a** Indexed X-ray diffraction pattern and, **b** scanning electron micrograph of BaTiO₃ templates produced by a two-stage molten salt (MSS) synthesis and topochemical microcrystal conversion method (TMC)

untransformed or residual phase from the three steps synthesis has not been observed. The morphology and the aspect ratio of the BT templates is another critical parameter in texturing of PMN-PT. From Fig. 2b the shapes of the templates were rectangular platelets with $\sim 1 \mu\text{m}$ homogeneous thicknesses. The actual lateral dimensions of the templates were calculated to be $\sim 6 \mu\text{m} \times 6 \mu\text{m}$ (length \times width) in average. However, it was observed and measured from SEM micrograph that there were some platelets with the same width and thicknesses but with approximately 5–12 μm length. The aspect ratio of templates was reported to be influential on the texturing of PMN-PT [3, 16, 27, 29]. The chemical composition and the shape of templates such as needle-like or plate-like are very important on the texturing [30, 31]. In this study, the dimensions of templates are compatible with required template dimension mentioned in one of the first studies in the literature [25].

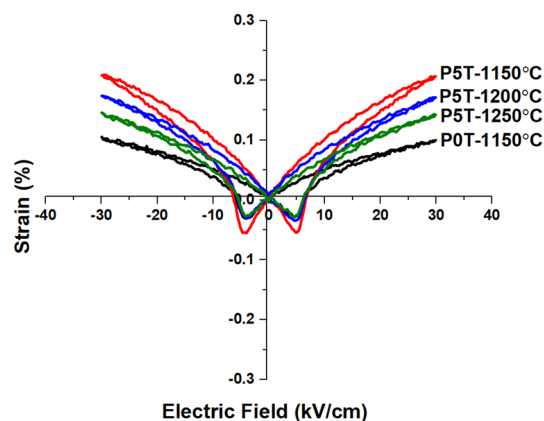


Fig. 3 Comparison of electric field induced bipolar strain curves of random PMN-PT and textured PMN-PT with 5 vol% BT templates sintered at different temperatures for 6 h

First, the sintering temperature study was done for P5T composition. Lotgering factors (f) of P5T composition sintered at 1150, 1200 and 1250 $^{\circ}\text{C}$ for 6 h were calculated as 0.90, 0.93 and 0.94, respectively. Electric field induced strain curves of these samples were given in Fig. 3. It was clearly seen from this figure taken at 30 kV/cm, that the highest strain level belongs to sample sintered at 1150 $^{\circ}\text{C}$. Piezoelectric charge coefficient (d_{33}) of P5T measured by Berlincourt method was recorded as 488, 416 and 369 pC/N for P5T samples sintered at 1150, 1200 and 1250 $^{\circ}\text{C}$, respectively. For a comparison, the d_{33} of the random POT sample sintered at 1150 $^{\circ}\text{C}$ for 6 h was measured by Berlincourt method as 270 pC/N. The ferroelectric properties of this POT sample sintered at 1150 $^{\circ}\text{C}$ were measured as; remnant polarization ($P_r \sim 17 \text{ pC/m}^2$) and maximum polarization ($P_{\text{max}} \sim 26 \text{ pC/m}^2$). There were no significant differences between the P_r and P_{max} values of random and textured samples sintered at these three different temperatures. The dielectric constant and dielectric loss of the P5T samples sintered at different temperatures have also been measured. The dielectric constants of the samples sintered at 1150, 1200 and 1250 $^{\circ}\text{C}$ were calculated as 1310, 1200 and 1072 with increasing dielectric loss, respectively. In summary, increasing the sintering temperature led to a decrease in the piezoelectric charge coefficient and the dielectric constant in addition to the increasing dielectric loss. The main reason of this decrease with increasing temperature is believed to be due to the increasing lead loss that occurs at higher sintering temperatures. Based on these measurement results, 1150 $^{\circ}\text{C}$ was selected as the optimum sintering temperature for P5T sample and this result is compatible with the literature [16], where 1150 $^{\circ}\text{C}$ was reported to be a sufficient temperature to develop texture at even short sintering durations [16, 27, 29].

After these initial investigations, the sintering treatment was also done under an oxygen rich atmosphere at 1150 $^{\circ}\text{C}$

for 6 h on a second set of samples. While the d_{33} value of the random P0T sample sintered in air was around 270 pC/N, it was found to have increased to 400 pC/N when it was sintered under oxygen atmosphere. This is a clear proof that the oxygen rich atmosphere had positive effect on the electrical properties and for the rest of study sintering was carried out under oxygen atmosphere. This positive effect is related to the densification behavior of the ceramics under oxygen rich atmosphere [32]. The atmospheric gas is entrapped within the isolated pores in the structure due to the lower diffusion of nitrogen through the perovskite lattice, whereas these isolated pores can easily be eliminated when the sintering is carried out under oxygen atmosphere because of the higher diffusion rate of oxygen through the perovskite lattice [33].

For further investigation, P1T, P3T and P5T samples were also sintered at 1150 °C for 6 h under oxygen atmosphere. XRD graph of these three samples was given in Fig. 4 and all peaks were indexed as the pseudocubic structure. All samples possess a pure perovskite structure without any secondary phase as shown in Fig. 4. Lotgering factor was calculated as 0.93, 0.93 and 0.96, for P1T, P3T and P5T samples sintered under oxygen atmosphere, respectively. When compared to the samples sintered in air, the texture as measured by the degree of grain orientation increased from 0.90 to 0.96 for P5T sample sintered at 1150 °C under oxygen. The (200) diffraction peak have also been investigated further by a detailed scan between 42° and 47° and the presence of multiple peaks have been observed. The rhombohedral PMN-PT is expected to yield a single diffraction peak for the (200) plane and the sub-peaklets are attributed to the tetragonal BT templates and the stress that they create on the matrix due to the lattice mismatch. A shorter sintering time of two hours have also been applied for all three barium titanate ratios while the sintering temperature was fixed at 1150 °C and the atmosphere was oxygen rich. Only a slight

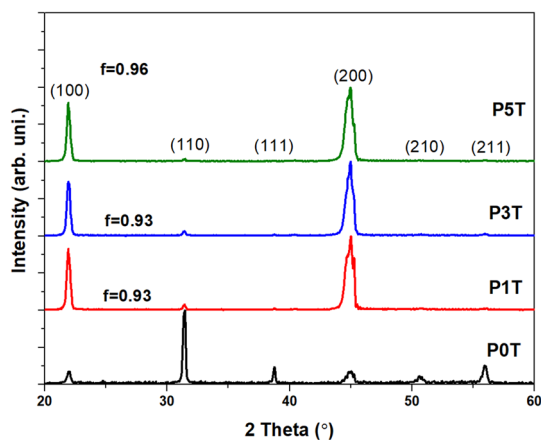


Fig. 4 Indexed X-ray diffraction patterns of random and textured PMN-PT samples sintered at 1150 °C for 6 h

difference in the Lotgering factor of the samples with changing sintering time was obtained because of similar grain size.

Electrical properties of PMN-PT were investigated with respect to BT template ratio and sintering time. Strain versus electric field graphs of P1T, P3T and P5T textured samples and random P0T samples sintered for 6 and 2 h were given in Fig. 5a, b, respectively. It was observed that the texture ratio of the P5T sample sintered at 1150 °C for 2 h was similar to the one sintered for 6 h, and their strain levels were also comparable. However, there were slight changes in the strain levels of P0T and P3T samples with sintering time. Shorter sintering time led to a slightly lower strain levels in P0T, whereas the strain levels increased in the case of P3T. However, a dramatic change has been observed in the strain level of P1T samples. There was an increase of 50% in the maximum strain level at 30 kV/cm from 0.2 to 0.3%. A similar trend was also observed in the piezoelectric and ferroelectric properties of P1T sample. Figure 6 is the brief graph of piezoelectric coefficient d_{33} and P_r of all of the samples with respect to BT template ratio and sintering

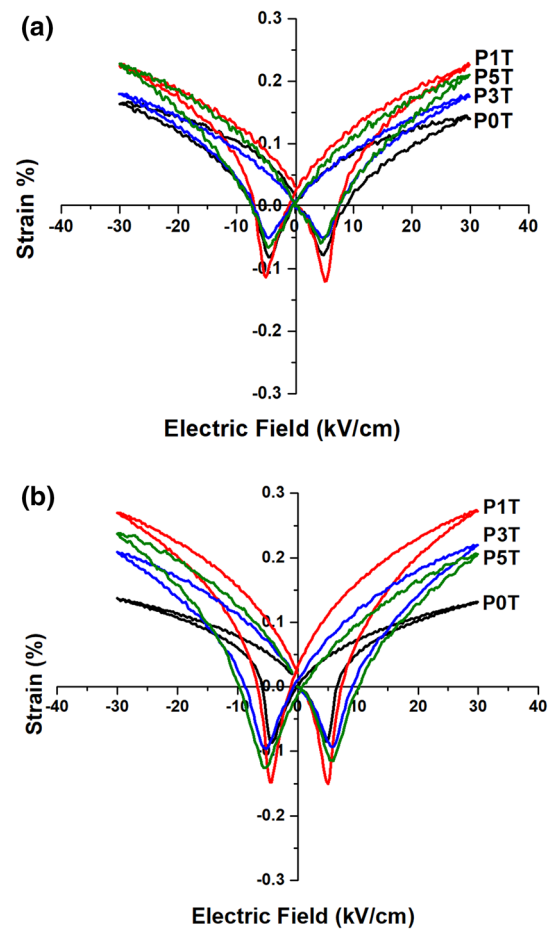


Fig. 5 Comparison of electric field induced bipolar strain curves of random and textured PMN-PT samples sintered at 1150 °C for **a** 6 h and **b** 2 h

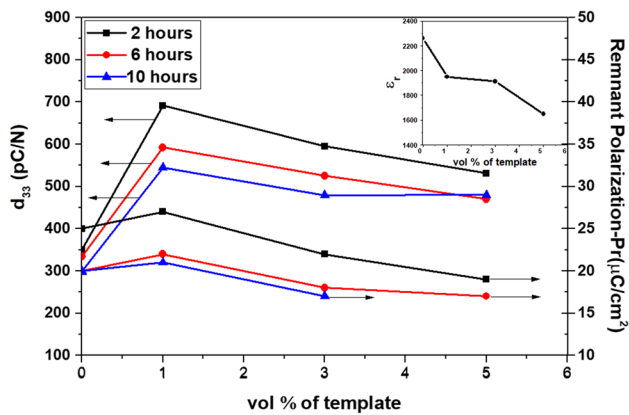


Fig. 6 Comparison of piezoelectric coefficient and remnant polarization values of PMN-PT samples with varying template content. Inset figure: variation of dielectric constant with varying template content

time. According to Fig. 6, d_{33} increased with decreasing sintering time for all samples. The same tendency was observed for all samples in the case of remnant polarization, as well. As a further confirmation, samples with various template contents have also been sintered at a longer time of 10 h, and as it is seen from Fig. 6, the d_{33} and P_r values of these samples were even lower than the 6 h sintered ones. The dielectric constant values of samples sintered at 1150 °C for 2 h were also calculated as a function of template ratio as seen in the inset figure of Fig. 6. Dielectric constants were found to decrease with increasing template ratio. When all of these results were evaluated; sintering time was found to be effective on the electromechanical properties of all samples, especially on P1T. The d_{33} of P1T increased from ~590 pC/N (10 h sintering) to ~700 pC/N (2 h sintering) with sintering time. The lower d_{33} that was observed at 10 h sintering is believed to be due to the increasing lead loss that is expected to occur at longer sintering times. This is consistent with the aforementioned trend of decreasing electromechanical properties with increasing sintering temperature. As an additional information, the high field converse piezoelectric coefficient d_{33}^* was also calculated from the unipolar strain measurements to be 733 pm/V for the P1T sample sintered at 2 h. In the literature, 5 vol% BT addition was usually preferred for texturing PMN-PT in various compositions by many researchers [3, 15, 35]. Lotgering factors of up to $f=0.96$ have been observed in those studies, where the d_{33} coefficients varying from 525 pC/N [35] to 630 pC/N [15] have been reported. Increasing the sintering time from 2 to 10 h was reported to have a limited effect on the texture and the electromechanical properties [3, 15]. However, in our study the processing conditions yielding the highest electrical and electromechanical properties are 1 vol% BT templates under sintering conditions of 1150 °C – 2 h, where $f=0.93$ and $d_{33}=700$ pC/N have been measured. In

the literature, lower template content have been studied by Yan et al. [3, 27], where the $f>0.95$ was reported to have been obtained from PMN-PT with 1 vol% BT templates and the $d_{33}=1000$ pC/N [27]. A lotgering factor of $f=0.77$ was reported to have been obtained from PMN-PT with 3 vol% BT templates and the $d_{33}\approx 520$ pC/N was measured. Thus, it can be concluded that the piezoelectric coefficients vary in a wide range for various template contents and sintering conditions, with sometimes contradicting trends, and the d_{33} values measured in our study are comparable to the literature and lie in the mid-range of the reported values. The reason of this variation in the properties are believed to lie in the differences that was observed in the morphology and aspect ratios of the BT templates, and the grain size of the PMN-PT matrix powder, all of which are the main parameters affecting the grain growth in the TGG process.

The descending tendency of d_{33} with respect to increasing template ratio can be explained in connection with the decrease of P_r , as seen from Fig. 6. Actually, decreasing of P_r value with increasing template ratio indicates that the domain motion is more difficult because of the clamping effect of barium titanate templates. Furthermore, related to these results, this clamping effect is also effective on the electromechanical properties. The clamping effect arises from the lattice mismatch between the PMN-PT matrix grains and the BT templates and this mismatch creates extra stresses, which affects the electromechanical properties such as d_{33} or strain. The clamping effect may also lead to a phase shift from the rhombohedral to the tetragonal structure. The PMN-PT composition that has been investigated in this study is actually in the rhombohedral region of the phase diagram. A rhombohedral ferroelectric composition oriented along the [001] direction would display much higher electromechanical properties compared to the [111] oriented counterpart. However, once the morphotropic phase boundary (MPB) is reached and passed towards the tetragonal side through compositional variation, the properties would decrease drastically [8]. In our case, the composition of the textured ceramic with 1 vol% BT templates is on the rhombohedral side of the MPB and oriented along the [001] direction, thus it is expected to exhibit high electromechanical properties. Increasing the BT template content further to 3 or 5 vol% would create an increased clamping effect and an increased volume of material would be under stresses arising from the interfaces between the textured grains and the BT templates. The tetragonal BT templates and the clamping effect may force a phase shift from the rhombohedral to the tetragonal phase, causing a further degradation in the electromechanical properties, as shown in the Fig. 6.

The dielectric loss ($\tan\delta$), dielectric constant and piezoelectric charge coefficient are also vital for the FOM in applications that require piezoelectrics with soft character. The changing of FOM and dielectric loss due to BT

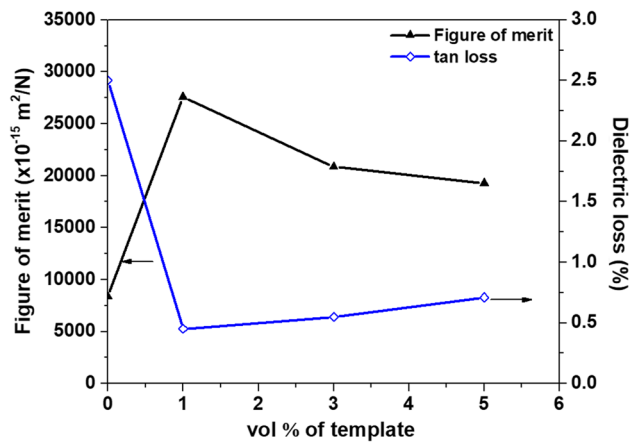


Fig. 7 Comparison of figure of merit and dielectric loss values of PMN-PT samples with varying template ratios

template ratio in PMN-PT samples sintered at 1150 °C for 2 h were shown in Fig. 7. The dielectric constants of these samples due to the increasing template ratio were found to be as 2260, 1950, 1913 and 1650 for P0T, P1T, P3T and P5T, respectively. According to Fig. 7, the FOM increases with the texture and achieves the maximum value of $\sim 27,500 \times 10^{-15} \text{ m}^2/\text{N}$ at 1 vol% BT template ratio. Beyond this template ratio, the FOM decreases consistently with d_{33} and ϵ_r . Additionally, $\tan\delta$ dramatically decreases and reaches its lowest value for the same template ratio. Since the desired system for energy harvesting applications requires piezoelectrics with high d_{33} and low dielectric loss and soft character, the PMN-PT textured with 1 vol% BT template was chosen as the ideal system.

Microstructural features of the samples were also examined by SEM. SEM micrographs of textured P1T sample were given in Fig. 8. The templates were clearly visible and were found to be well aligned in the PMN-PT matrix. The grain sizes of the samples were measured as $\sim 10 \mu\text{m}$. Both surface and cross sectional views of microstructure indicated a dense ceramic. Grain boundaries were also clearly visible, and identified with white arrows on the micrograph. When compared to some of the studies [16, 27, 29] in the literature that have reported high electrical properties with higher degree of texture, the main difference in our study was the slightly thicker templates. The thicknesses of the templates were measured as 1.0–1.3 μm . These dimensions indicated a lower aspect ratio in the templates compared to the previously reported studies, and this explains some of the differences that were observed in the electrical properties. Grain size and template ratio are very effective on the degree of the texture and on the electrical properties. Since the BT template particles remain intact after the high temperature annealing process with very limited diffusion, the microstructure of the textured ceramic, with the mixture of

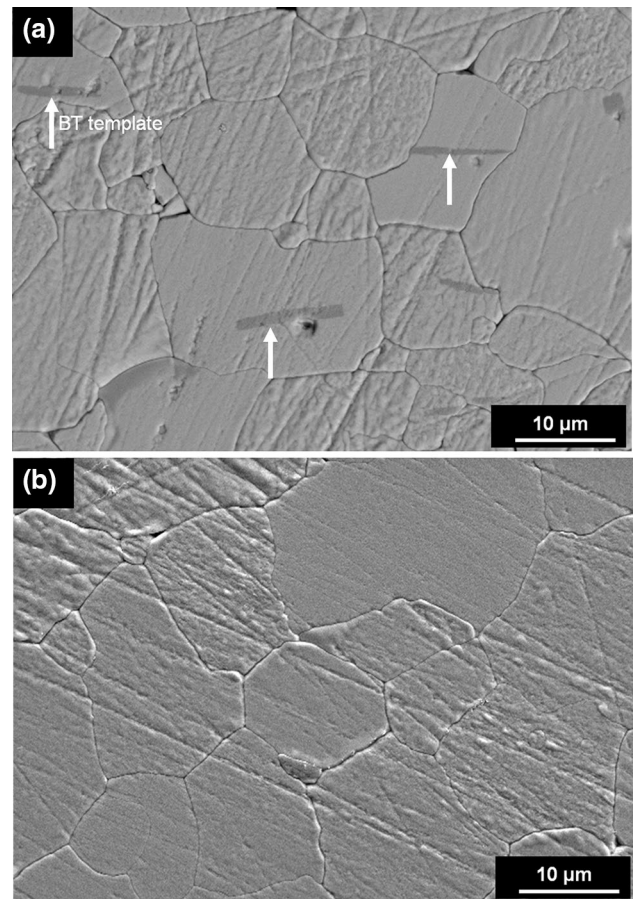


Fig. 8 **a** Cross-sectional and **b** surface scanning electron microscope micrographs of PMN-PT sample textured with 1 vol% BT templates (P1T)

matrix and template grains, can be considered as a composite consisting of template grains with low dielectric and electromechanical properties embedded in a matrix with high dielectric and electromechanical properties. It was reported in the literature [27, 29] that properties started to decrease after a critical ratio of template content. It was another reason that in the current study, sample with 1 vol% BT had higher electromechanical properties and higher BT template content led a decrease in the properties.

3.2 Temperature dependence of dielectric and impedance properties

The dielectric constant of random P0T and textured P1T samples as a function of temperature was measured at 1 kHz, 10 and 100 kHz. Neither of the samples exhibit relaxor characteristic (not shown here). The comparison of the dielectric constants with respect to temperature at 10 kHz for both random P0T and P1T samples was shown in Fig. 9. From binary phase diagram of PMN-PT, it is known that there is a phase transition from rhombohedral FE to tetragonal FE

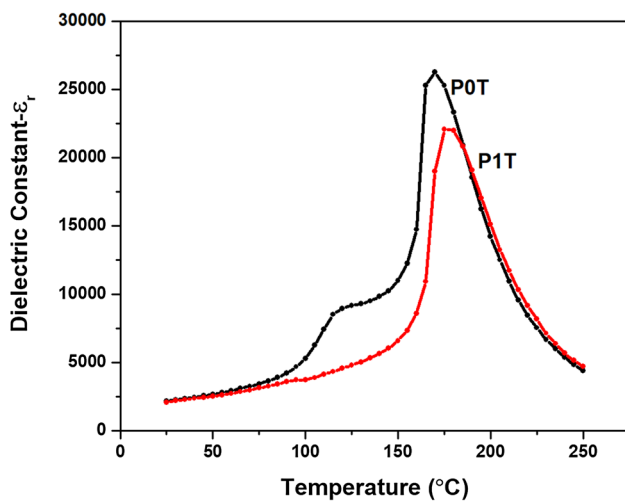


Fig. 9 The variation of dielectric constant with temperature of random (POT) and textured PMN-PT samples (PIT)

phase at low temperatures. In this study, this transition was observed only for poled random POT sample and the phase transition temperature (T_{R-T}) was measured as ~ 120 °C. Another phase transition, from tetragonal ferroelectric phase to cubic paraelectric phase, was also observed at the Curie temperature- T_c , of 170 °C. The maximum value of dielectric constant at T_c was also found to be as $\epsilon_{r-max} \sim 26,260$ at 10 kHz. These values are comparable to the literature on PMN-PT with 1 mol% PbO excess [16, 34]. It was reported that these peaks of T_{R-T} and T_{max} shift with increasing PbO in the PMN-PT structure [16]. The addition of PbO may cause formation of intergranular phases with low- ϵ (dielectric permittivity) and additionally point defects in the structure. The presence of these intergranular imperfections may then lead to formation of stresses and stabilize the space-charge field around the grains, which would then “lock-in” the ferroelectric polarization, allowing the dipoles to persist to higher than normal temperatures [16].

The dielectric constant as a function of temperature for poled textured PIT (containing 1 vol% BT sample with 2 wt% PbO) was also seen in Fig. 9. The first phase transition, the monoclinic to tetragonal phase transition- T_{M-T} , for textured PIT sample could not clearly be identified as random sample. A very weak slope change was observed around 100 °C. The suppression of the FE-FE phase transition can also be attributed to the clamping effect of BT templates. The stresses arising from this effect may stabilize one FE phase and suppress the transition to the other FE phase. The Curie temperature- T_c of textured sample was identified as 180 °C. Thus, it is concluded that barium titanate that is present in the microstructure did not have a drastic effect on the value of T_c compared to random PMN-PT. However, the peak value of the dielectric constant of the textured sample

decreased remarkably compared to random one and found to be $\epsilon_{r-max} \sim 22,070$ at 10 kHz. This decrease may be attributed to the mixing of BT phase or Pb vacancies as a secondary dielectric phase in PMN-PT or presence of large grains in the textured sample [16]. As a supporting result, when BT content was increased to 3 vol%, the T_c was measured to be 180 °C, but the peak value of ϵ_r was further decreased to 17,805 at 10 kHz (not shown here). Additionally, the monoclinic-tetragonal transition has not been observed in the 3 vol% BT containing textured sample either.

As it has been discussed in the previous sections, the dielectric loss is an important parameter in the energy harvesting applications, and since the AC conductivity is one of the components of the loss, it was investigated through impedance spectroscopy. Impedance spectroscopy analyses were done for further investigation of the effect of texture on to the electrical properties of PMN-PT, such as resistivity and conductivity. Comparison of real (Z') and imaginary (Z'') parts of impedance measurements of random POT and textured PIT samples with identical sizes taken at 300 and 500 °C, as a function of frequency (f) were given in Fig. 10. It is seen from Fig. 10a, b that the magnitude of imaginary part of impedance, Z'' , decreases with increasing temperature for both samples. This indicates that the AC conductivity increased with increasing temperatures [36]. The magnitude of Z' also decreases with increasing temperature for both random and textured samples (not shown here). The levels of decrease of Z' and Z'' were almost one to two orders of magnitude for every 100 °C increment of the temperature. As it was seen from Fig. 10a, b, the level of Z'' increased three orders of magnitude between 300 and 500 °C for both samples. This means conductivity increased drastically with temperature for both samples. Although these increment values between the temperatures are faster than lead-free potassium sodium niobate (KNN), the levels of impedance are lower than KNN [20] and KNN added other systems [37]. This means conductivity level for PMN-PT system is higher than the KNN system.

When the peaks are compared with each other for both random and textured samples, the peak point of the textured sample at 500 °C was observed at a lower frequency compared to random one. The peak was found at 4.8×10^4 Hz with an impedance value of 1.57 k Ω for textured sample, whereas it was observed at 6.8×10^5 Hz with an impedance value of 0.17 k Ω for random sample. The observation of the maxima of the peak at higher frequency, leading to shorter relaxation times, indicates a higher presence of oxygen vacancies. Same tendency was also observed at 300 °C but the peak of the textured sample could not be observed because of the frequency limitation of our system.

Another remarkable result is that the levels of Z' and Z'' especially at the peak points for the textured PIT sample were almost one order of magnitude higher than that of the

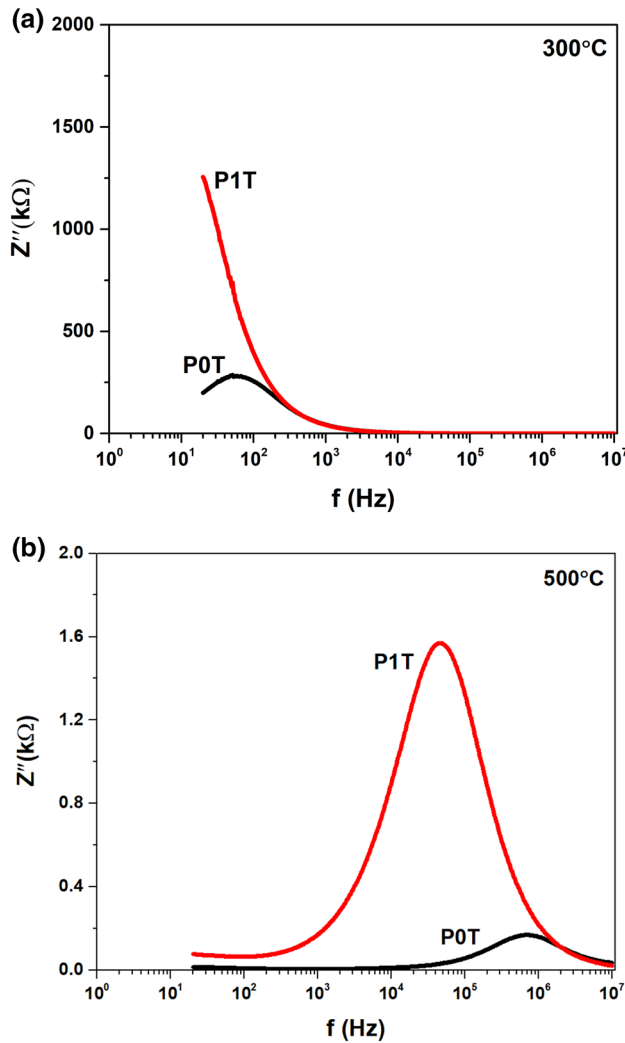


Fig. 10 Variations of imaginary part of impedance of random (P0T) and textured PMN-PT samples (P1T) at **a** 300 °C and **b** 500 °C

random P0T sample. This result shows that texturing or BT addition led to a decrease in AC conductivity. Conductivity is a second rank tensor property and depending on the symmetry of the crystalline phases, conductivity can be represented with two coefficients in the case of tetragonal and rhombohedral crystals and with four coefficients in the case of monoclinic crystals. This indicates that there will be an anisotropy in the properties and the conductivity will be inherently higher in certain crystallographic directions. Although, this is valid for single crystals, a crystallographically textured ceramic will also display this anisotropy in the conductivity. A randomly oriented polycrystalline ceramic, on the other hand, will be isotropic and the conductivity can be represented with a single coefficient, which would be an average of the coefficients in various directions, and thus would be lower than the single crystal values in certain directions. One of the reasons of the observed difference in

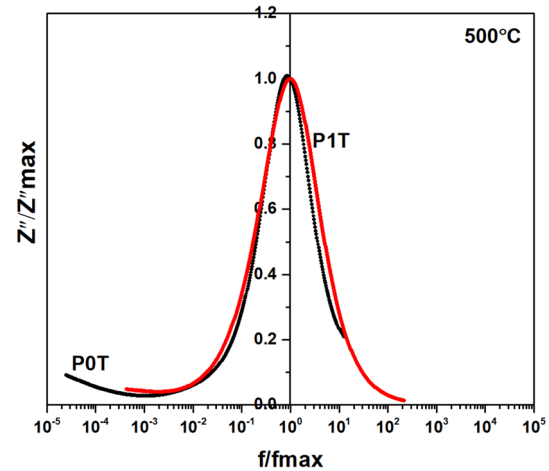


Fig. 11 Variation of the normalized imaginary parts (Z''/Z''_{\max}) of impedance as a function of normalized frequency (f/f_{\max}) in the random and textured samples at 500 °C

the conductivity of the textured and random ceramics is this anisotropy. Beside this, the difference of the characteristics of the grain boundaries in the textured and random structures is believed to be effective for conductivity.

It can be also seen from Fig. 10 that Z'' plots as a function of different frequencies show broad peaks depending on the measurement temperature. This implies that the relaxation is temperature-dependent, and that a single relaxation time does not exist for either of the samples. The peak maximum also indicates relaxation frequency. As the temperature was increased, in addition to the expected decrease in magnitude of Z'' , there is a shift in the peak frequencies towards the high frequency side for each sample. Beside this, the Z'' peaks of random and textured samples merged at above 100 Hz at 300 °C and merged above 1 MHz at 500 °C for both samples. These results mean that, the peaks shifts towards higher frequencies by increasing temperature and then finally merge, suggesting the accumulation of space charge in PMN-PT [38].

The normalized imaginary parts (Z''/Z''_{\max}) of impedance as a function of normalized frequency (f/f_{\max}) in the random and textured samples at 500 °C were also given in Fig. 11. Z''/Z''_{\max} data exhibited almost symmetric peaks with broadening for both random and textured samples at this temperature. A slight difference of peak broadening was due to the existence of different relaxation times for the samples.

For further investigation, the complex impedance Cole–Cole plots (Nyquist diagrams) at 300 and 500 °C are given in Fig. 12a, b for both random and textured samples, respectively. It is seen from Fig. 12 that neither of the samples have a semicircle at 300 °C while these samples have full but slightly depressed semicircles at 500 °C. A perfect semicircle with center on the Z' -axis should be observed for

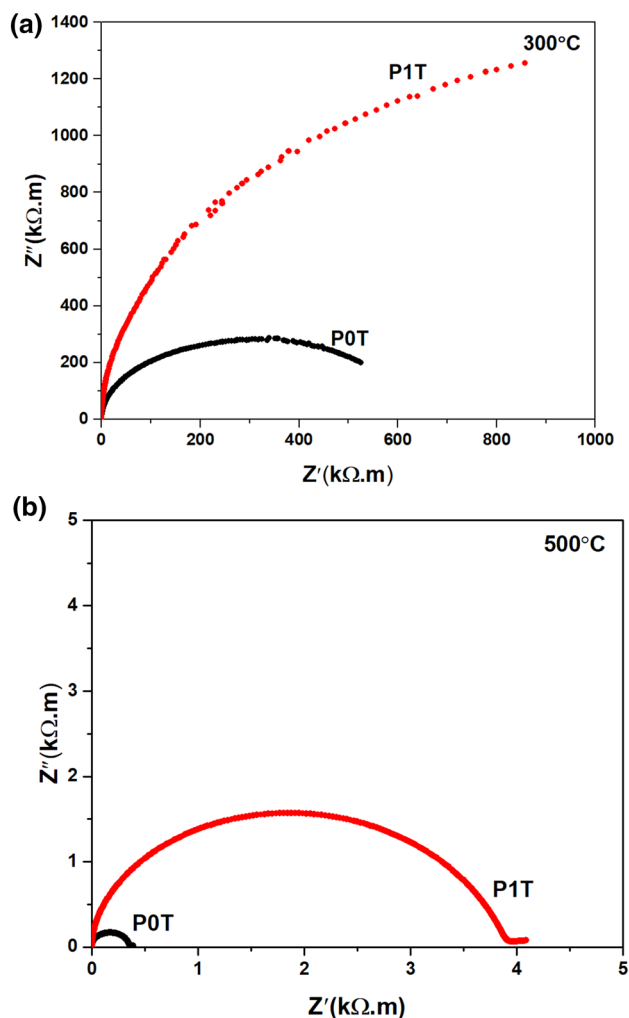


Fig. 12 The Cole–Cole plots of the random and textured samples at **a** 300 °C and **b** 500 °C

ideal Debye-type relaxation. Actually, depressed semicircle indicates non-Debye-type relaxation thus a distribution of relaxation time will be obtained [39, 40]. The Cole–Cole plots at 500 °C can be resolved to have a main, high-frequency semicircle and a tail at low frequencies, which is actually the onset of a second semicircle. The one in the low-frequency regime can be attributed to the grain boundary effects or the onset of a purely resistive conductivity, while the high-frequency semicircle corresponds to the bulk relaxation.

4 Conclusion

Textured $0.675\text{Pb}(\text{Mg}_{1/3}\text{Nb}_{2/3})\text{O}_3\text{-}0.325\text{PbTiO}_3$ ceramics were investigated for energy harvesting applications with an aim to obtain high FOM, high piezoelectric coefficient, relatively low dielectric constant and low dielectric loss. In this

study, the ceramics textured using 1 vol% BT and sintered at 1150 °C for 2 h under oxygen atmosphere were selected as the optimum. FOM increases with the texture and achieves the maximum value of $\sim 27,500 \times 10^{-15} \text{ m}^2/\text{N}$ at 1 vol% BT template ratio. The Curie temperature- T_c of textured sample was also measured as 180 °C and there was no clear FE–FE phase transition at lower temperature due to the suppression of the FE–FE phase transition, which was attributed to the clamping effect of BT templates. Impedance spectroscopy was done for random and textured PMN-PT samples. Texturing and BT addition led to a decrease in the AC conductivity. The peak was found at 4.8×10^4 Hz with an impedance value of 1.57 kΩ for textured sample and the peak was observed at 6.8×10^5 Hz with an impedance value of 0.17 kΩ for random sample. The observation of the maxima of the peak at higher frequency indicates a higher presence of oxygen vacancies in the random sample.

Acknowledgements The authors wish to acknowledge the financial support of Turkish Academy of Sciences (Gebip Programme) and TUBITAK Project #217M086. The authors also would like to thank Prof. Sedat Alkoy and Prof. Huseyin Yilmaz for fruitful discussions.

References

1. G. Shirane, S. Hoshino, J. Phys. Soc. Jpn. **6**, 265 (1951)
2. B. Jaffe, W.R. Cook Jr., H. Jaffe, *Piezoelectric Ceramics* (Academic Press, London, 1971), p. 135
3. Y. Yan, K.H. Cho, S. Priya, J. Am. Ceram. Soc. **94**, 1784 (2011)
4. R.A. Islam, S. Priya, Appl. Phys. Lett. **88**, 032903 (2006)
5. S.S. Chandratreya, R.M. Fulrath, J.A. Pask, J. Am. Ceram. Soc. **64**, 422 (1981)
6. B. Noheda, J.A. Gonzalo, L.E. Cross, R. Guo, S.E. Park, D.E. Cox, G. Shirane, Phys. Rev. B **61**, 8687 (2000)
7. R.E. Newnham, *Properties of Materials: Anisotropy, Symmetry, Structure* (Oxford University Press, New York, 2004)
8. S.E. Park, T.R. Shrout, J. Appl. Phys. **82**, 1804 (1997)
9. S.E. Park, T.R. Shrout, IEEE Trans. Ultrason. Ferroelectr. Freq. Control **44**, 1140 (1997)
10. N. Yamamoto, Y. Yamashita, Y. Hosono, K. Itsumia, Sens. Actuators A **200**, 16 (2013)
11. S. Zhang, F. Li, J. Appl. Phys. **111**, 031301 (2012)
12. G.L. Messing, S. Trolier-McKinstry, E.M. Sabolsky, C. Duran, S. Kwon, B. Brahmaroutu, P. Park, H. Yilmaz, P.W. Rehrig, K.B. Eitel, E. Suvaci, M. Seabaugh, K.S. Oh, Crit. Rev. Solid State Mater. Sci. **29**, 45 (2004)
13. K.T. Zawilski, M.C.C. Custodio, R.C. DeMattei, S.-G. Lee, R.G. Monteiro, H. Odagawa, R.S. Feigelson, J. Cryst. Growth **258**, 353 (2003)
14. Y. Chang, Y. Sun, J. Wu, X. Wang, S. Zhang, B. Yang, G.L. Messing, W. Cao, J. Eur. Ceram. Soc. **36**, 1973 (2016)
15. T. Richter, S. Denzler, C. Schuh, E. Suvaci, R. Moss, J. Am. Ceram. Soc. **91**, 929 (2008)
16. E.M. Sabolsky, S. Trolier-McKinstry, G.L. Messing, J. Appl. Phys. **93**, 4072 (2003)
17. K.H. Brosnan, Processing, properties, and application of textured $0.72\text{Pb}(\text{Mg}_{1/3}\text{Nb}_{2/3})\text{O}_3\text{-}0.28\text{PbTiO}_3$ ceramics. Ph.D Dissertation, The Pennsylvania State University, University Park, PA, 2007

18. S.F. Poterala, S. Trolier-McKinstry, R.J. Meyer, G.L. Messing, J. Appl. Phys. **110**, 014105 (2011)
19. N.V. Prasad, M.C. Sekhar, G.S. Kumar, Ferroelectrics **366**, 55 (2008)
20. E. Mensur Alkoy, A. Berksoy-Yavuz, IEEE Trans. Ultrason. Ferroelectr. Freq. Control **59**, 2121 (2012)
21. E. Mensur-Alkoy, A. Berksoy-Yavuz, S. Alkoy, Ferroelectrics **447**, 95 (2013)
22. M.A.L. Nobre, S. Lafredi, Catal. Today **78**, 529 (2003)
23. N. Hirose, A. West, J. Am. Ceram. Soc. **79**, 1633 (1996)
24. S.L. Swartz, T.R. Shrout, Mater. Res. Bull. **17**, 1245 (1982)
25. D. Liu, Y. Yan, H. Zhou, J. Am. Ceram. Soc. **90**, 1323 (2007)
26. S. Dursun, Ultrasonic motor applications of crystallographically textured piezoceramics. Ph.D. Dissertation, Gebze Technical University, Kocaeli, Turkey, 2017
27. Y. Yan, Y.U. Wang, S. Priya, Appl. Phys. Lett. **100**, 192905 (2012)
28. F.K. Lotgering, J. Inorg. Nucl. Chem. **9**, 113–123 (1959)
29. Y. Yan, L. Yang, Y. Zhou, K.-H. Cho, J.S. Heo, S. Priya, J. Appl. Phys. **118**, 104101 (2015)
30. G. Feng, H. Rong-zi, L. Jia-ji, Y. Yong-hong, T. Chang-sheng, Eur. Ceram. Soc. **28**, 2063 (2008)
31. S. Alkoy, S. Dursun, IEEE Trans. Ultrason. Ferroelectr. Freq. Control **60**(10), 2044 (2013)
32. S. Kwon, E.M. Sabolsky, G.L. Messing, J. Am. Ceram. Soc. **84**, 648 (2001)
33. Y. Yoshikawa, K. Tsuzuki, J. Am. Ceram. Soc. **75**(9), 2520 (1992)
34. E.M. Sabolsky, A.R. James, S. Kwon, S. Trolier-McKinstry, G.L. Messing, Appl. Phys. Lett. **78**(17), 2551–2553 (2001)
35. Y. Cheng, J. Wu, Y. Sun, S. Zhang, X. Wang, B. Yang, G.L. Messing, W. Cao, Appl. Phys. Lett. **107**, 082902 (2012)
36. S.M. Gupta, P. Pandit, P. Patro, A.J. Kulkarni, V.K. Wadhawan, Mater. Sci. Eng. B **120**, 194 (2005)
37. J. Ji, B. Fang, X. Zhao, S. Zhang, Q. Du, J. Ding, H. Luo, J. Mater. Sci. Mater. Electron. **29**, 4422 (2018)
38. K. Lily, K. Kumari, K. Prasad, R.N.P. Choudhary, J. Alloys Compd. **453**, 325 (2008)
39. B. Behera, P. Nayak, R.N.P. Choudhary, J. Alloys Compd. **436**, 226 (2007)
40. B. Pati, R.N.P. Choudhary, P.R. Das, B.N. Parida, R. Padhee, J. Electr. Mater. **42**, 1225 (2013)